7404–7415 Nucleic Acids Research, 2012, Vol. 40, No. 15 Published online 8 May 2012
doi:10.1093/nar/gks330

Rapid incorporation kinetics and improved fidelity of a novel class of 3′-OH unblocked reversible terminators

Andrew F. Gardner[1], Jinchun Wang[2], Weidong Wu[2], Jennifer Karouby[1], Hong Li[2], Brian P. Stupi[2], William E. Jack[1], Megan N. Hersh[2] and Michael L. Metzker[2,3,4,*]

[1]New England Biolabs, Ipswich, MA 01938, [2]LaserGen, Inc., Houston, TX 77054, [3]Human Genome Sequencing Center and [4]Department of Molecular and Human Genetics, Baylor College of Medicine, Houston, TX 77030, USA

Received January 19, 2012; Revised March 30, 2012; Accepted April 3, 2012

ABSTRACT

Recent developments of unique nucleotide probes have expanded our understanding of DNA polymerase function, providing many benefits to techniques involving next-generation sequencing (NGS) technologies. The cyclic reversible termination (CRT) method depends on efficient base-selective incorporation of reversible terminators by DNA polymerases. Most terminators are designed with 3′-*O*-blocking groups but are incorporated with low efficiency and fidelity. We have developed a novel class of 3′-OH unblocked nucleotides, called *Lightning Terminators*™, which have a terminating 2-nitrobenzyl moiety attached to hydroxymethylated nucleobases. A key structural feature of this photocleavable group displays a 'molecular tuning' effect with respect to single-base termination and improved nucleotide fidelity. Using Therminator™ DNA polymerase, we demonstrate that these 3′-OH unblocked terminators exhibit superior enzymatic performance compared to two other reversible terminators, 3′-*O*-amino-TTP and 3′-*O*-azidomethyl-TTP. *Lightning Terminators*™ show maximum incorporation rates (k_{pol}) that range from 35 to 45 nt/s, comparable to the fastest NGS chemistries, yet with catalytic efficiencies (k_{pol}/K_D) comparable to natural nucleotides. Pre-steady-state kinetic studies of thymidine analogs revealed that the major determinant for improved nucleotide selectivity is a significant reduction in k_{pol} by >1000-fold over TTP misincorporation. These studies highlight the importance of structure–function relationships of modified nucleotides in dictating polymerase performance.

INTRODUCTION

DNA polymerases belong to at least seven families [A, B, C, D, X, Y and reverse transcriptase (RT)] that display a wide range of cellular roles, replicative fidelities and propensities toward incorporating modified nucleotide substrates or natural nucleotides across damaged templating bases (1–5). For example, high-fidelity DNA polymerases have a remarkable ability to copy their genomes with high accuracy. For DNA polymerases in general, a major factor contributing to the degree of replicative fidelity is nucleotide selectivity; that is, the ability for a DNA polymerase to correctly choose the right nucleotide substrate over the wrong one. The capacity by which a DNA polymerase performs this selection process occurs by recognizing at least two differences in the nucleotide structure: (i) sugar selectivity (i.e. an OH group versus an H atom at the 2′-position of ribose) and (ii) nucleobase selectivity (i.e. geometric shape of the Watson–Crick versus mismatched base-pairs).

Despite low sequence conservation, there is a striking similarity in the overall structural architecture among many polymerase families, reminiscent of a half-opened right hand containing the fingers, palm and thumb domains (6,7). Protein sequence alignment for polymerase members belonging to Families A, B and RT have revealed two highly conserved regions, motif A and motif C, which participate in nucleotide binding and the phosphoryl transfer reaction within the fingers and palm domains of the active site (8). Key amino acid residue(s) within motif A of DNA polymerases belonging to these families have been shown to act as a 'steric gate' to discriminate against the incorporation of ribonucleotides by a structural clash with the 2′-OH group (9–15). Interestingly, mutational analysis of amino acid residues involving or immediately surrounding the steric gate region of motif A have also revealed lower DNA synthesis fidelity (16–19) and an

*To whom correspondence should be addressed. Tel: +1 713 798 7565; Fax: +1 713 798 5741; Email: mmetzker@bcm.edu
Present address:
Jennifer Karouby, InvivoGen, San Diego, CA 92121, USA.

increased capability to extend synthesis beyond mismatched incorporated bases (20). Nucleobase discrimination is thought to involve a tight fit of the overall geometric shape of the correct Watson–Crick base-pair within the *closed* active site to promote the fast catalytic activity of DNA polymerase (4,21–24). Thus, the relaxation of sugar selectivity may be coupled with lower fidelity by having a looser fit that accommodates larger geometric shapes of mismatched base-pairs in the *closed* active site.

Easing of this otherwise structural stringency with appropriate steric gate variants is not limited to the 2′-position of nucleotides. For example, DNA polymerases with several steric gate variants have also been shown to improve the incorporation of 2′,3′-dideoxynucleoside-5′-triphosphates (2′,3′-ddNTPs) (12,25). These 2′,3′-ddNTPs have been widely used in Sanger sequencing (26) and served as the initial basis to develop another class of nucleotide terminators, 3′-*O*-modified reversible terminators (27,28). These 3′-*O*-blocked nucleotides are currently being used in several next-generation sequencing (NGS) technology approaches by employing the cyclic reversible termination (CRT) method (29,30), which involves single-base incorporation, fluorescent imaging to identify the just incorporated base, and removal of the terminating and fluorescent dye moieties to restore the 3′-OH group. A number of 3′-*O*-modified reversible terminator chemistries have been developed with labile blocking groups such as 3′-*O*-amino (31,32), 3′-*O*-azidomethyl (33,34), 3′-*O*-allyl (27,35,36) and 3′-*O*-nitrobenzyl (36,37). A major challenge with this approach has been to identify appropriate DNA polymerases that can incorporate the 3′-*O*-modified nucleotide with the desired properties of fast nucleotide-incorporation kinetics and high nucleotide selectivity (30).

Our group was the first to demonstrate that a small 2-nitrobenzyl group attached to the N^6-position of dATP created an effective reversible terminator with wild-type *Bst* DNA polymerase (37). Upon photochemical cleavage with 365 nm ultraviolet (UV) light, this 2-nitrobenzyl-modified dATP analog is transformed back into its corresponding natural nucleotide form. While this 3′-OH unblocked nucleotide was a promising reversible terminator, translation of this approach to an N^3-modified thymidine analog was predicted and confirmed to adversely affect nucleotide-incorporation fidelity. This prompted development of novel 2-nitrobenzyl-modified thymidine analogs based on 5-hydroxymethyl-2′-deoxyuridine-5′-triphosphate (HOMedUTP), a naturally found hypermodified nucleotide (38).

We have demonstrated a 'molecular tuning' effect by increasing the size of the alkyl group attached to the α-methylene carbon of the 2-nitrobenzyl group to confer unique properties such as high nucleotide selectivity and single-base termination with two commercially-available DNA polymerases, Therminator and Vent(exo$^-$) (38). The 3′-OH unblocked analog 5-[(*S*)-1-(2-nitrophenyl)-2,2-dimethyl-propyloxy]methyl-dUTP (dU.V) was identified as an efficient reversible terminator by repeated cycles of stepwise incorporation and photochemical cleavage through a homopolymer repeat of ten complementary templating bases (38) using the CRT method (29,30). A complete set of 3′-OH unblocked reversible terminators based on 7-deaza-7-hydroxymethyl-2′-deoxyadenosine-5′-triphosphate (C^7-HOMedATP), 5-hydroxymethyl-2′-deoxy cytidine-5′-triphosphate (HOMedCTP) and 7-deaza-7-hydroxymethyl-2′-deoxy-guanosine-5′-triphosphate (C^7-HOMe-dGTP) has now been developed, called *Lightning Terminators*™. We have demonstrated that the stereospecific *S* configuration of an α-*tert*-butyl group and the ring modification of a 5-OMe group are important determinants in providing fast photochemical cleavage kinetics (39). To further explore the unique properties of these 3′-OH unblocked reversible terminators, we have now characterized the pre-steady-state kinetic basis of 5′-hydroxymethyl-2′-deoxyuracil (HOMedU) analog dU.V and its 5-OMe substituted analog 5-[(*S*)-1-(5-methoxy-2-nitrophenyl)-2,2-dimethyl-propyloxy]methyl-dUTP (dU.VI, Figure 1A), having the properties of fast nucleotide-incorporation kinetics, high nucleotide selectivity and single-base termination. We present evidence that these 3′-OH unblocked reversible terminators exhibit superior enzymatic performance properties when compared with two 3′-*O*-blocked reversible terminators, namely 3′-*O*-amino-TTP and 3′-*O*-azidomethyl-TTP (Figure 1B) using Therminator DNA polymerase. Remarkably, the other nucleotide members of the *Lightning Terminators*™ set (i.e. dA.VI, dC.VI and dG.VI, Figure 1C) show fast nucleotide-incorporation kinetics similar to its thymidine counterpart.

MATERIALS AND METHODS

DNA polymerases and nucleic acids

9°N-7(exo$^-$) DNA polymerase is a Family B DNA polymerase, cloned from the *Thermococcus* species 9°N-7, and contains the D141A and E143A variants causing 3′→5′ exonuclease deficiency (40). Therminator DNA polymerase is 9°N-7(exo$^-$) that also contains the A485L variant (41). Therminator III DNA polymerase is 9°N-7(exo$^-$) DNA polymerase that also contains the L408S, Y409A and P410V variants. Therminator, Therminator III and Klenow(exo$^-$) DNA polymerases, along with TTP, were obtained from New England Biolabs, Inc. (Ipswich, MA, USA). HOMedUTP (38) was purchased from TriLink BioTechnologies, Inc. (San Diego, CA, USA). 3′-*O*-amino-TTP (31) was purchased from Firebird Biomolecular Sciences, LLC (Gainesville, FL, USA). Other nucleotide analogs were synthesized as previously described: 3′-*O*-azidomethyl-TTP (33,42), 5-[(*S*)-1-(2-nitrophenyl)-2,2-dimethyl-propyloxy]methyl-dUTP (dU.V) (38) and 7-[(*S*)-1-(5-methoxy-2-nitrophenyl)-2,2-dimethyl-propyloxy]methyl-7-deaza-dATP (dA.VI), 5-[(*S*)-1-(5-methoxy-2-nitrophenyl)-2,2-dimethyl-propyloxy]methyl-dCTP (dC.VI), 7-[(*S*)-1-(5-methoxy-2-nitrophenyl)-2,2-dimethyl-propyloxy]methyl-7-deaza-dGTP (dG.VI) and 5-[(*S*)-1-(5-methoxy-2-nitrophenyl)-2,2-dimethyl-propyloxy]methyl-dUTP (dU.VI) (39). Oligonucleotides were purchased from Integrated DNA Technologies, Inc. (Coralville, IA, USA).

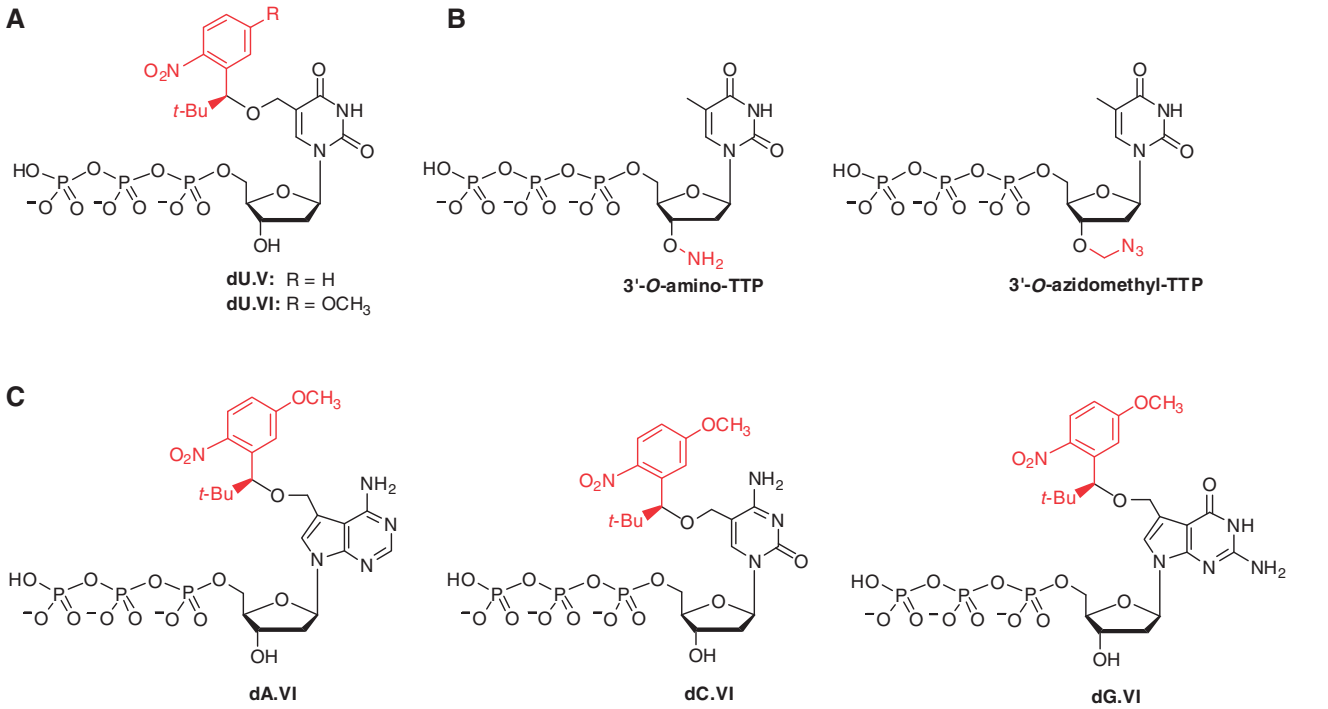

Figure 1. Chemical structures of (**A**) 3′-OH unblocked reversible terminators: dU.V and dU.VI, (**B**) 3′-*O*-modified reversible terminators: 3′-*O*-amino-TTP and 3′-*O*-azidomethyl-TTP and (**C**) 3′-OH unblocked reversible terminators: dA.VI, dC.VI and dG.VI. Red chemical structures denote terminating functional groups that cleave when exposed to (A and C) UV light or (B) sodium nitrite or tris(2-carboxyethyl)phosphine, respectively.

Purification of modified nucleotides

All thymidine nucleotides except for 3′-*O*-amino-TTP were purified by reverse-phase high performance liquid chromatography (RP–HPLC) as previously described (38,39), followed by enzymatic 'Mop-Up' to remove contaminating TTP or HOMedUTP (43). A successful mop-up was determined by the elimination of an otherwise +2 DNA product when assayed against a homopolymer repeat template at a final nucleotide concentration of 10 μM and an incubation time of 10 min using Therminator DNA polymerase. Eliminating TTP contamination from the 3′-*O*-amino-TTP stock proved difficult as these nucleotides comigrate by RP–HPLC, consistent with that noted by Benner (44). As 3′-*O*-amino-TTP is incorporated by many commercially-available DNA polymerases (32), we devised a solution-based, kinetic mop-up assay using Therminator DNA polymerase by incubating the reaction at 65°C for 1 min. This is based on the premise that the incorporation rate of TTP is faster than that of 3′-*O*-amino-TTP and short incubation times would effectively remove much of the contaminating natural nucleotide. The 3′-*O*-azidomethyl-TTP analog was purified three times by RP–HPLC followed by the kinetic mop-up assay to remove contaminating TTP. Following a single round of RP–HPLC, bead-based mop-up assays were performed using Klenow(exo$^-$) DNA polymerase as the mop-up enzyme for dU.V and dU.VI (43). In all cases, mopped-up solutions were separated from the magnetic beads (bead-based method), passed through an Amicon Ultra-0.5 centrifugal 10 000 molecular weight cut-off (MWCO) filter (Millipore, Billerica, MA, USA) to remove mop-up polymerase and primer/template duplex, and placed on ice in the dark.

The other *Lightning Terminators*™ (dA.VI, dC.VI and dG.VI) were also purified by RP–HPLC, but were not subjected to the mop-up assay as these purified samples were determined to be free of natural nucleotide contamination by incorporation assays, as described above.

Polymerase end-point assays using correct and mismatched templating bases

Polymerase end-point (PEP) assays for incorporation (correct) and nucleotide selectivity (mismatched) experiments were performed as previously described (37,38). Incorporation reactions were analyzed on a 10% polyacrylamide gel using an Applied Biosystems (AB), now Life Technologies (Foster City, CA, USA) model 377 DNA sequencer and informative fluorescence peaks were quantified manually.

Burst kinetics assays

FAM-duplex DNA-A was formed by mixing equimolar amounts of the 6-carboxyfluorescein-labeled primer, 5′-AGTGAATTCGAGCTCGGTACCCGGGGATCCTCTAGAGTCGACCTGCAGGC, with the template-A, 5′-TTGCTCGTTTGCTGGGAGCCTGCAGGTCGACTCTAGAGGATCCCCGGGTACCGAGCTCGAATTCACT, (interrogation base underlined) in 1× ThermoPol Buffer [20 mM Tris–HCl, 10 mM $(NH_4)_2SO_4$, 10 mM KCl, 2 mM $MgSO_4$, 0.1% Triton X-100, pH 8.8] and then by heating to 95°C for 5 min, followed by annealing the duplex at

60°C for 10 min, and cooling to room temperature over a 15 min period. FAM-duplex DNA-C, -G and -T were also assayed by replacing template-A with template-C, 5′-AAGTATGAAAGTAGGGCGCCTGCAGGTCGAC TCTAGAGGATCCCCGGGTACCGAGCTCGAATTC ACT, template-G, 5′-CCCTAATCATATCCTGGGCCT GCAGGTCGACTCTAGAGGATCCCCGGGTACCG AGCTCGAATTCACT, or template-T, 5′-AAGCACG AAAGCAGGGTGCCTGCAGGTCGACTCTAGAG GATCCCCGGGTACCGAGCTCGAATTCACT, respectively (interrogation base underlined).

Burst kinetic experiments were employed to determine the rate limiting step qualitatively. Rapid-quench reactions were carried out as described below by mixing 40 µl of 80 nM FAM-duplex DNA-A containing 20 nM Therminator DNA polymerase in 1× ThermoPol buffer with 40 µl of either 50 µM dU.V or dU.VI or 200 µM TTP or HOMedUTP in 1× ThermoPol buffer. FAM duplex DNA -C, -G, or -T reactions were similarly carried out with 50 µM dG.VI, dC.VI, or dA.VI, respectively. The reactions were allowed to proceed for pre-determined time points and then were quenched by addition of 200 µl of 0.5 M Na_2EDTA. Time point increments that ranged from 3 ms to 10 s were performed using an RQF-3 rapid-quenched-flow instrument (Kintek Corp., Austin, TX, USA). Initial time points >10 s were performed manually. All Therminator or Therminator III DNA polymerase reactions were analyzed at 60°C due to constraints of the RQF-3 instrument. Incorporation reactions were analyzed using an AB model 3730xl capillary analyzer. Fluorescence peaks were quantified and analyzed using Peak Scanner Software v1.0 (AB).

The burst amplitude (A), burst rate (k_{burst}) and observed steady-state rate (k_{SS}') were fitted using a non-linear least squares approach from the equation (45,46):

$$[\text{product}] = A[1 - \exp(-k_{burst}t) + (k_{SS}')t]$$

The normalized rate constant (k_{SS}) was then calculated by dividing k_{SS}' by A, having the units of nanomolar product formed per second per nanomolar active enzyme.

Pre-steady-state kinetic experiments

Single turnover nucleotide-incorporation reactions were performed by rapidly mixing 40 µl of 25 nM of Therminator DNA polymerase containing 10 nM FAM-duplex DNA-A in 1× ThermoPol buffer together with 40 µl of nucleotides or nucleotide analogs at appropriate concentrations in 1× ThermoPol buffer. As described above, reactions proceeded for pre-determined time points, quenched with Na_2EDTA and analyzed using an AB model 3730xl DNA capillary analyzer.

The first-order rate constant (k_{obs}) for incorporation reactions for each nucleotide concentration was calculated by plotting the natural log of the remaining substrate versus time. Rate constants (k_{obs}) were then plotted as a function of nucleotide or analog concentration and fitted to the hyperbolic equation:

$$k_{obs} = (k_{pol}[\text{nucleotide}]/K_D + [\text{nucleotide}])$$

where k_{pol} is the maximum rate of nucleotide addition and K_D is the nucleotide ground state binding equilibrium constant (47).

Termination experiments

4,4-Difluoro-5,7-dimethyl-4-bora-3a,4a-diaza-*s*-indacene-3-propionic acid (BODIPY-FL) duplex DNA-E was formed by mixing 40 nM of template-E, 5′-CCGACGTA CGTAAACTGGCCGTCGTTTTACAGCCGCCGCCG CCGAACCGA-Biotin, (interrogation bases underlined) with 5 nM of BODIPY-FL-labeled primer R931 (48), 5′-CTGTAAAACGACGGCCAG-s-T, (where 's' is a phosphorothioate linkage) in 1× ThermoPol buffer and then by heating to 80°C for 30 s, followed by annealing the duplex at 57°C for 30 s, and then cooling to 4°C. The duplex was then diluted in half (its final concentration was 2.5 nM in a volume of 10 µl) by the addition of 94 nM Therminator DNA polymerase in 1× ThermoPol buffer. After heating at 65°C for 30 s, 1 µl of 100 µM dU.V or dU.VI was added. Incorporation reactions were rapidly mixed and incubated at 65°C for 0.5, 1, 2, 3, 4, 5, 10 and 20 min time increments, quenched with 10 µl of stop solution (98% deionized formamide; 10 mM Na_2EDTA, pH 8.0; 25 mg/ml Blue Dextran, MW 2 000 000) and then placed on ice in the dark. Termination reactions were analyzed using an AB model 377 DNA sequencer, and informative fluorescence peaks were quantified manually.

RESULTS

Reversible terminators used in NGS technologies

The performance of the reversible terminator plays a critical role in cycle time and data quality for NGS systems (30). We recently described a novel set of 3′-OH unblocked terminators based on 2-nitrobenzyl-modified HOMedU nucleotides that were efficiently incorporated using either Vent(exo$^-$) or Therminator DNA polymerases (38). For the current study, we chose Therminator DNA polymerase as it has been reported to be more tolerant to incorporating sugar-modified nucleotides belonging to the general classes of acyclic (41,49), ring-modified (50,51) and 3′-*O*-blocked (32) analogs. Thus, to characterize performance differences between 3′-*O*-blocked and 3′-OH unblocked terminators, we describe detailed enzymatic studies using Therminator DNA polymerase comparing the HOMedU analogs dU.V (38) and dU.VI (39) along with the thymidine analogs 3′-*O*-amino-TTP (31,32) and 3′-*O*-azidomethyl-TTP (33,34); see Figure 1A and B. Additionally, the other *Lightning Terminators*, dA.VI, dC.VI and dG.VI, (Figure 1C) were also tested to evaluate potential differences between nucleobase analogs.

A challenge of utilizing reversible terminators in NGS technologies is the presence of contaminating natural nucleotides (29). DNA polymerases generally discriminate against modified nucleotides in favor of their natural nucleotide counterparts when presented as a mixture. We refer to this property as the incorporation bias (37). This is important as interpretation of the results obtained from enzymatic experiments can be confounded when even

trace amounts of natural contamination are present. It has been our experience that the majority of reversible terminator preparations, obtained by in-house synthesis or commercial sources, contain significant quantities (i.e. ≤0.5%) of contaminating natural nucleotides even after RP–HPLC purification (43). Therefore, the four thymidine/HOMedU analogs were purified by repeated RP–HPLC and/or Mop-Up assay (43) to eliminate contaminating TTP or HOMedUTP below detectable levels when assayed at a final nucleotide concentration of 10 μM, prior to performing the experiments described below.

Reduced incorporation bias with 3′-OH unblocked *Lightning Terminators*™

Initially, we performed the PEP assay (37) to measure the incorporation bias, expressed as the ratio of IC_{50} values (i.e. the nucleotide concentration at which the number of moles of the primer equals that of the incorporated product) for the modified nucleotide over the natural nucleotide using Therminator DNA polymerase. Compared with the IC_{50} value of HOMedUTP, dU.V and dU.VI each showed a slight incorporation bias of 2.9 and 4.3, respectively (Table 1). The incorporation bias for 3′-*O*-amino-TTP was 9.0 and 10.1 compared with TTP and HOMedUTP, respectively. The bias for 3′-*O*-amino-TTP was >2-fold higher compared to either 3′-OH unblocked terminator despite that the (*S*)-α-*tert*-butyl-2-nitrobenzyl group being substantially larger in size (Figure 1A and B). This comparison highlights the adverse effect of attaching even a small functional group such as NH_2 to the 3′-*O* position of the nucleotide. This point is emphasized further with the modified TTP analog containing the larger 3′-*O*-azidomethyl group, which was not incorporated at all by Therminator DNA polymerase up to a final concentration of 10 μM (data not shown). These data are consistent with the inverse relationship of increasing size at the 3′-*O*-position and decreasing incorporation performance of Therminator DNA polymerase (i.e. –OH > $–ONH_2$, >> $–OCH_2N_3$).

PEP assays were also performed with dA.VI, dC.VI and dG.VI and compared with the corresponding native nucleotides C^7-HOMedATP, HOMedCTP and C^7-HOMedGTP, respectively (Table 1), each revealing a lower incorporation bias (range 1.0–3.5) compared with that of dU.VI. These data highlight that low incorporation bias is an intrinsic property of *Lightning Terminators*™.

Lightning Terminators™ exhibit fast nucleotide-incorporation rates and higher binding affinities

We next performed pre-steady-state kinetic experiments to determine the constants k_{pol} and K_D for TTP, HOMedUTP, dU.V, dA.VI, dC.VI, dG.VI and dU.VI. Unfortunately, at concentrations >10 μM, TTP contamination could not be efficiently removed from the 3′-*O*-amino-TTP solution and given its incorporation bias of ~10-fold, it was not characterized further.

An incorporation event can be expressed by the following simplified kinetic reaction:

$$E+DNA_n = E \bullet DNA_n + dNTP \overset{K_D}{\longleftrightarrow}$$

$$E \bullet DNA_n \bullet dNTP \overset{k_{pol}}{\longrightarrow} E \bullet DNA_{n+1} \bullet PP_i$$

where K_D is the ground state nucleotide binding equilibrium constant and k_{pol} is the maximum rate of incorporation, which encompasses both the conformation change from the *open* to *closed* state (k_2) and the phosphoryl transfer chemistry step (k_3) (4).

Pre-steady-state kinetic studies were performed with Therminator DNA polymerase in molar excess over the primer/template duplex. Molar excess was verified by repeating these experiments at a 2-fold higher Therminator DNA polymerase concentration, which did not alter either k_{pol} or K_D constants (data not shown). The kinetic constants, k_{pol} and K_D, for TTP and HOMedUTP were similar to those for dCTP (45) using the related archaeal DNA polymerases, Vent(exo$^-$) and Vent(exo$^-$) A488L variant, the latter of which contains the amino acid substitution analogous to that found in Therminator DNA polymerase (Table 2). For the 3′-OH unblocked analogs, dU.V and dU.VI, k_{pol} rate constants were $37 \pm 6\,s^{-1}$ and $36 \pm 7\,s^{-1}$, respectively, which are ~5- to 7-fold slower than their natural nucleotide counterparts. The maximum rate constants for dA.VI, dC.VI and dG.VI

Table 1. PEP assay results using Therminator DNA polymerase

Nucleotide	IC_{50} (nM)	Incorporation bias
TTP[a]	1.9 ± 0.1	N/A
HOMedUTP[a]	1.7 ± 0.1	N/A
dU.V[a]	4.9 ± 0.2	2.9
dU.VI	7.3 ± 0.6	4.3
3′-*O*-amino-TTP	17.1 ± 1.7	9.0
3′-*O*-azidomethyl-TTP	No Incorp.	N/A
C^7-HOMedATP	1.0 ± 0.1	N/A
dA.VI	3.5 ± 0.1	3.5
HOMedCTP	1.5 ± 0.1	N/A
dC.VI	1.5 ± 0.1	1.0
C^7-HOMedGTP	2.1 ± 0.1	N/A
dG.VI	2.8 ± 0.2	1.3

[a]IC_{50} data obtained from Litosh *et al.* (38).

Table 2. Pre-steady-state kinetic constants using Therminator DNA polymerase

Nucleotide	k_{pol} (s^{-1})	K_D (μM)	k_{pol}/K_D ($\mu M^{-1}\,s^{-1}$)	Selection (analog/TTP)
TTP	170 ± 4	73 ± 3	2.3	1.0
HOMedUTP	250 ± 11	33 ± 7	7.6	3.3
dU.V	37 ± 6	15 ± 2	2.5	1.1
dA.VI	45 ± 1	4.0 ± 0.1	11	ND
dC.VI	36 ± 1	8.7 ± 1.1	4.1	ND
dG.VI	35 ± 1	16 ± 3	2.2	ND
dU.VI	36 ± 7	12 ± 1	3.0	1.3

The nucleotide concentration range used in these studies were 5–1000 μM for TTP, 25–1000 μM for HOMedUTP and 1–50 μM for dU.V, dA.VI, dC.VI, dG.VI and dU.VI. ND indicates that kinetic parameters for their corresponding natural nucleotides were not determined.

were very similar to that of their hydroxymethyluracil counterparts (Table 2). The binding constants (K_D) for dU.V and dU.VI were ~2 to 6-fold lower than those for TTP and HOMedUTP, suggesting higher binding affinities of the 3′-OH unblocked terminators within the Therminator active site. Similar ground state binding constants were observed for dA.VI, dC.VI and dG.VI (Table 2). Of the four *Lightning Terminators*, dA.VI showed the fastest k_{pol} rate constant and lowest K_D binding constant of the nucleotide set.

The pre-steady-state kinetic parameter (k_{pol}/K_D) can be used to express the catalytic efficiency of a given nucleotide or nucleotide analog (47). The catalytic efficiencies of the *Lightning Terminators*™ ranged from 2.2 to 11 μM^{-1} s^{-1} similar to those of TTP and HOMedUTP, Table 2. These data provide good evidence that the 3′-OH unblocked hydroxymethyluracil terminators are as efficient in catalytic performance as the natural nucleotide TTP and strongly suggest that the other *Lightning Terminators*™ would show similar catalytic performance with their corresponding native nucleotides.

Lightning Terminators™ exhibit fast burst kinetics

To further characterize the enzymatic performance of 3′-OH unblocked terminators, burst kinetic experiments were performed with the primer/template duplex in excess of Therminator DNA polymerase. For natural nucleotides, previous burst studies have shown biphasic kinetics of an initial fast turnover rate, called the burst rate (k_{burst}), occurring at the active site of polymerase, followed by a slower steady-state rate (k_{SS}) that is dependent on the duplex dissociating from polymerase. Therminator DNA polymerase displayed the biphasic burst pattern similar to those for Klenow fragment (52), AmpliTaq CS (53), RB69 (54), Vent(exo$^-$) and Vent(exo$^-$) A488L (45), *Sso* PolB1(exo$^-$) (55) and *Pfu*(exo$^-$) (56) DNA polymerases. The rapid burst rates (k_{burst}) were $146 \pm 60\,s^{-1}$ and $130 \pm 9\,s^{-1}$ followed by slow steady-state turnover rates (k_{SS}) of $0.03 \pm 0.01\,s^{-1}$ and $0.07 \pm 0.01\,s^{-1}$ for TTP and HOMedUTP, respectively; see Supplementary Figure S1A and B. The burst amplitude (A) was measured from these curves, indicating that ~90% of the Therminator DNA polymerase preparation was active. Remarkably, the *Lightning Terminators* dA.VI, dC.VI, dG.VI and dU.VI (Figure 2) and dU.V (Supplementary Figures S1C) also displayed a biphasic burst pattern similar to that for natural nucleotides. The rapid burst rates (k_{burst}) ranged from $24 \pm 9\,s^{-1}$ to $51 \pm 30\,s^{-1}$ followed by slow steady-state turnover rates (k_{SS}) that ranged from $0.02 \pm 0.01\,s^{-1}$ to $0.06 \pm 0.01\,s^{-1}$ (Table 3).

Slow mismatch incorporation rate governs improved nucleotide selectivity for dU.V and dU.VI

To maintain replication fidelity, DNA polymerases have evolved mechanisms for exquisite selectivity to insert the correct nucleotide across its complementary templating

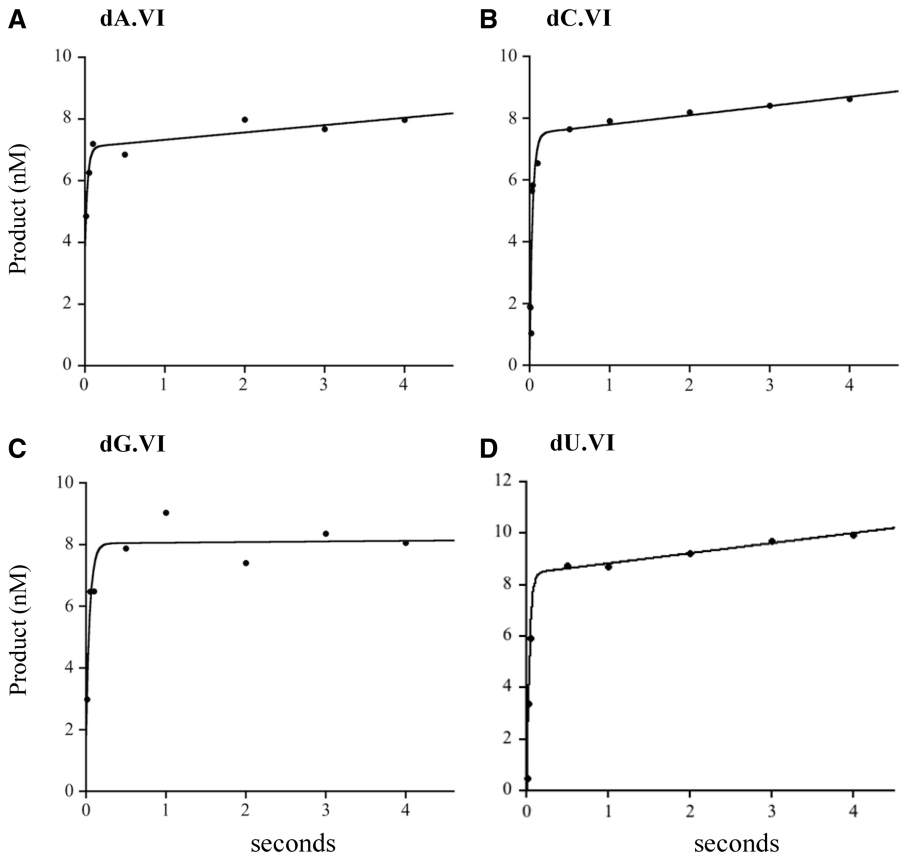

Figure 2. Burst kinetics plots of (**A**) dA.VI, (**B**) dC.VI, (**C**) dG.VI and (**D**) dU.VI. See experimental section for details.

base. For example, we previously reported that the nucleotide selectivity for Vent(exo$^-$) polymerase showed greater than three orders of magnitude difference in IC_{50} values for correctly inserting TTP over misincorporating it against mismatched templating bases (38). Substitution with variant amino acid residues in regions other than the steric gate can also affect synthesis fidelity of DNA polymerases. For example, nucleotide selectivity ratios using Therminator DNA polymerase containing the A485L variant were lower for TTP by two orders of magnitude than with Vent(exo$^-$) DNA polymerase (38). For 2-nitrobenzyl-modified 3′-OH unblocked HOMedU analogs, alkyl groups of increasing size on the α-methylene carbon of the 2-nitrobenzyl group improve nucleotide selectivity of Therminator DNA polymerase (38). PEP mismatched assays were performed for dU.VI, which revealed the similar findings of improved nucleotide selectivity over TTP (Table 4). To define the kinetic parameters that govern nucleotide selectivity, we examined the misincorporation of TTP, dU.V and dU.VI, opposite dCMP, dGMP and TMP in the template strand using Therminator DNA polymerase.

Table 3. Burst kinetic constants using Therminator DNA polymerase

Nucleotide	k_{burst} (s^{-1})	k_{SS} (s^{-1})
TTP	146 ± 60	0.03 ± 0.01
HOMedUTP	130 ± 9	0.07 ± 0.01
dU.V	24 ± 9	0.02 ± 0.01
dA.VI	51 ± 30	0.03 ± 0.01
dC.VI	35 ± 10	0.05 ± 0.01
dG.VI	38 ± 14	0.06 ± 0.01
dU.VI	33 ± 9	0.02 ± 0.01

Table 4. Nucleotide selectivity results for TTP and dU.VI using Therminator DNA polymerase

Template base	IC_{50}	
	TTP[a]	dU.VI
A	1.9 ± 0.1 nM	7.3 ± 0.6 nM
C	20 ± 3 nM	4.3 ± 0.3 μM
G	42 ± 3 nM	3.0 ± 0.2 μM
T	84 ± 1 nM	3.9 ± 0.1 μM

[a]IC_{50} data obtained from Litosh *et al.* (38).

Consistent with our previous data, Therminator DNA polymerase readily misincorporates across all mismatched templating bases when TTP is the only nucleotide provided (Table 5). Rates of maximum incorporation (k_{pol}) for TTP were slightly lower for mismatched templating bases (range 1.8- to 3.0-fold) than for the correct templating base. The nucleotide ground state binding constant (K_D) for mismatches showed slightly weaker binding affinity (range 2.1- to 4.7-fold) compared to the correct templating base. From these kinetic constants, nucleotide selectivity can be expressed as a discrimination ratio D of $k_{pol}/K_{D(correct)}$ divided by $k_{pol}/K_{D(mismatch)}$ (4). D ratios for TTP:dCMP, TTP:dGMP and TTP:TMP mismatches were only 4.9, 14 and 7.0, respectively, which are in strong agreement with those ratios using the PEP nucleotide selectivity assay (38); see Table 5.

To explore the kinetic basis for improved nucleotide selectivity of dU.V and dU.VI, we performed pre-steady-state experiments. Unlike that of TTP, k_{pol} constants for dU.V and dU.VI were substantially lower for mismatched templating bases compared to that of the correct templating base (range 720- to 1270-fold and 570- to 1030-fold, respectively). Across the same mismatched templating base, k_{pol} constants for dU.V and dU.VI were more than three orders of magnitude lower than that of TTP. On the other hand, differences in ground state binding constant (K_D) with mismatched templating bases showed only slightly weaker binding affinity (range 0.8- to 2.8-fold and 1.1- to 3.7-fold, respectively). D ratios for dU.V and dU.VI against mismatched templating bases ranged from 630 to 2000 and 620 to 2900, respectively, which were generally higher than those ratios using the PEP nucleotide selectivity assay; see Table 5. These data suggest that the major determinant for improved nucleotide selectivity for dU.V and

Table 5. Nucleotide selectivity using pre-steady-state and PEP assays using Therminator DNA polymerase

Nucleotide	Template base	k_{pol} (s^{-1})	K_D (μM)	k_{pol}/K_D (μM^{-1} s^{-1})	Nucleotide selectivity	
					k_{pol}/K_D (Corr.)/k_{pol}/K_D (MisM)	IC_{50} (MisM)/ IC_{50} (Corr.)
TTP[a]	C	72 ± 1	150 ± 8	0.48	4.9	11
	G	55 ± 2	340 ± 50	0.16	14	22
	T	97 ± 4	290 ± 19	0.33	7.0	44
dU.V[a]	C	0.045 ± 0.035	12 ± 2	3.8×10^{-3}	630	1300
	G	0.030 ± 0.002	25 ± 1	1.2×10^{-3}	2000	740
	T	0.053 ± 0.011	45 ± 4	1.2×10^{-3}	2000	850
dU.VI[b]	C	0.063 ± 0.020	13 ± 3	4.8×10^{-3}	620	590
	G	0.048 ± 0.016	44 ± 6	1.1×10^{-3}	2800	400
	T	0.035 ± 0.010	34 ± 10	1.0×10^{-3}	2900	540

[a]IC_{50} data can be found in Litosh *et al.* (38).
[b]IC_{50} data can be found in Table 4.
Corr., correct template base; MisM, mismatched template base.

dU.VI is a significant reduction in the maximum incorporation rate (k_{pol}).

Tert-butyl-2-nitrobenzyl modified HOMedUTP analogs exhibited single-base termination in homopolymer repeats

A challenge in using 3′-OH unblocked terminators is creating appropriate modification(s) to the terminating group so that DNA synthesis is stopped after a single-base addition. As the 3′-OH group is the appropriate substrate, incorporating the next incoming nucleotide or nucleotide analog is possible with the effect of reading through the target templating base and causing type 1 dephasing (i.e. the primer has advanced beyond the target templating base) of the primary signal (30). If observed, the rate $k_{pol(+2)}$ for the second base incorporation can be measured to determine the extent of the nucleotide read-through. For example, Bowers *et al*. described pre-steady-state kinetics employing two-base homopolymer templates, for which $k_{pol(+2)}$ rates were measured for all of their 3′-OH unblocked 'virtual' terminators (57).

We recently reported that the size of the α-substitution group plays an important role in 'tuning' the termination properties of 2-nitrobenzyl alkylated HOMedUTP analogs (38). Therefore, we performed pre-steady-state kinetic experiments using a two-base 'AA' homopolymer template for dU.V and dU.VI. Unlike that of Bowers et al. who conducted their termination experiments at submicromolar nucleotide concentrations (i.e. from 100 to 250 nM), termination assays were performed at 10 μM over the time course of 0.5 to 20 min. Both dU.V and dU.VI (Figure 3) were rapidly incorporated at the first base position (100% by 2 min) and then terminated DNA synthesis at that position. We could not detect any appreciable signal at the expected second-base position up to incubation times of 20 min. Single-base termination was verified by gel electrophoresis, which showed that the DNA products of photochemical cleavage comigrated with that of a singly incorporated TTP nucleotide (compare lanes Ct and Pc). Thus, we were unable to measure $k_{pol(+2)}$ rates for either analog, indicating that dU.V and dU.VI are efficient at single-base termination for homopolymer template sequences.

DISCUSSION

In this study, we performed a direct comparison of 3′-OH unblocked and 3′-*O*-modified terminators using Therminator DNA polymerase, previously shown to incorporate a variety of sugar-modified (32,41,49,51) and base-modified (37,38) nucleotides. Incorporation biases of modified nucleotides appear to be governed more by the site to which the terminating group is attached rather than its molecular size, as both 3′-OH unblocked nucleotides (dU.V and dU.VI) having a much larger terminating group showed less bias than 3′-*O*-amino-TTP. A key advantage of the 3′-OH unblocked *Lightning Terminators*™ is their fast nucleotide-incorporation rates. Remarkably, the *Lightning Terminator*™ analogs also exhibited a characteristic biphasic burst pattern, which is not observed with many modified nucleotide substrates (45,53). We attribute this superior performance in enzyme kinetics primarily to having an unblocked 3′-OH group. To further highlight this point, we characterized 3′-*O*-azidomethyl-TTP with Therminator III DNA polymerase, which contains numerous variants in the steric gate region: L408S, Y409A and P410V. Unlike the results for Therminator, 3′-*O*-azidomethyl-TTP was incorporated by Therminator III. Pre-steady-state kinetic experiments revealed a maximum rate of incorporation (k_{pol}) to be $0.68 \pm 0.04\,s^{-1}$ and the nucleotide ground state binding constant (K_D) to be $7.1 \pm 0.1\,\mu M$. Thus, even under optimized conditions

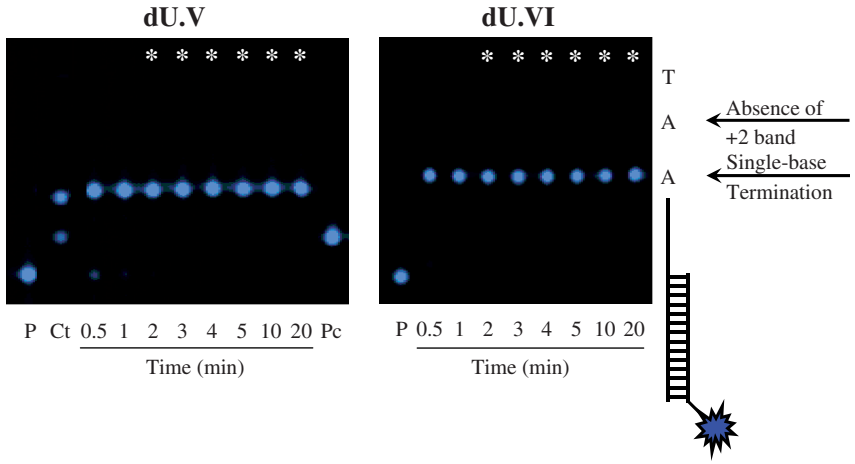

Figure 3. Single-base termination of dU.V and dU.VI. Therminator DNA polymerase was bound to primer/template complex in 1× Thermopol buffer and subjected to 10 min incubation at 75°C in HPLC water (lane 'P' or primer), 50 nM TTP (lane 'Ct' or control) or 10 μM dU.V followed by a 90 s exposure to 365 nm UV light (lane 'Pc' or photochemical cleavage)—control lanes demonstrating that the incorporation bands of dU.V and dU.VI are the result of a single-base incorporation event. The remaining lanes represent incubation time courses of 10 μM dU.V or 10 μM dU.VI. Prior to performing the termination assays, dU.V and dU.VI were purified using the mop-up assay to remove trace amounts of HOMedUTP (43). Weighted-sum analysis was performed, yielding a value = 1.0 (white asterisks) at time points from 2 to 20 min (38). We note that the weighted-sum method, which has been reported previously (38), is used to measure quantitatively the termination property of nucleotide analogs being extended along a homopolymer stretch of complementary template bases. The slightly slower mobility of dU.VI termination products over those of dU.V results from the higher mass of the OMe group. Assays were performed in triplicate, a representative gel of which is shown.

involving the relaxation of the steric gate residues, the incorporation rates for the *Lightning Terminators*™ were still faster by >50-fold.

Crystal structures of the apo enzyme for many Family B polymerases have been determined including 9°N-7 (58), D. Tok (59), KOD1 (60), *Pfu* (61), RB69 (62), *Sso* PolB1 (63) and *Tgo* (64). As the ternary structure of RB69 bound with a primer/template duplex and TTP has also been solved (65), these amino acid coordinates can serve as a model for other hyperthermophilic DNA polymerases, including Therminator. For example, the 2′-deoxyribose group of the incoming TTP stacks on top of the phenolic ring of a conserved tyrosine group at amino acid position 416 (Y416), corresponding to the Y409 residue in Therminator and DNA polymerase. The 3′-OH group of TTP is positioned to make hydrogen bonds to the –NH group of the peptide bond for Y409 and to its non-bridging oxygen of the β-phosphate group. Figure 4A illustrates a model whereby the 3′-OH group of dU.VI is hydrogen bonding with these groups. This model is supported by kinetic data showing that the absence of 3′-OH group for nucleotide terminators, such as 2′,3′-ddNTPs, disrupts hydrogen bonding to these functional groups and lowers k_{pol} by 400- to 1100-fold in Vent(exo$^-$) and RB69 DNA polymerases, respectively (45). Figure 4B illustrates a model whereby 3′-*O*-azidomethyl-TTP disrupts hydrogen binding and the 3′-*O*-modification causes steric clashing with one or more amino acid residues within the active site, providing an explanation for its non-incorporation by Therminator polymerase. In the present study, k_{pol} constants for dU.V and dU.VI were only slightly lower (5- and 7-fold) than TTP or HOMedUTP, respectively and dA.VI, dC.VI and dG.VI showed similar rate constants to dU.V and dU.VI. These data suggest that the (*S*)-*tert*-butyl-2-nitrobenzyl group has only a modest adverse effect on the kinetic properties of these reversible terminators.

Lightning Terminators™ dU.V and dU.VI show higher nucleotide binding affinities (i.e. lower K_D constants) than TTP for both correct (Table 2) and mismatched (Table 5) base-pairs. This finding suggests that the hydrophobic (*S*)-*tert*-butyl-2-nitrobenzyl group may bind favorably within the active site of Therminator DNA polymerase, independent of the templating base. We note that the fold differences, however, in ground state nucleotide binding constants for correct and mismatched base-pairs were similar for TTP (range 2.1- to 4.7-fold), dU.V (range 0.8- to 2.8-fold) and dU.VI (range 1.1- to 3.7-fold). These data suggest that Therminator DNA polymerase is a weak discriminator for nucleotide binding of mismatched base-pairs that is independent of the substrates tested here. Despite the overall structural similarities, Joyce and Benkovic provide good evidence that even members of the same DNA polymerase family show extreme variability in the 'kinetic checkpoint' of weak versus strong discrimination for ground state binding (24).

In contrast to ground state binding, we observed substantial differences in the maximum rate of incorporation (k_{pol}) across the same mismatched base-pairs, with dU.V or dU.VI being lower by >1100-fold compared to TTP. Thus, our data support the model that the mismatched discrimination of dU.V and dU.VI occurs after ground state nucleotide binding. As k_{pol} measures both finger closing (k_2) and phosphoryl transfer chemistry (k_3) steps, we cannot assign the degree to which either or both are reduced. Recently, we reported that increasing the size of the α-substitution group has a direct relationship by improving discrimination between correct and mismatched incorporation (38). With this in mind, we favor a model in which the rate of closing the fingers domain around the nucleotide (k_2) is reduced, as steric clash between the group on the α-carbon and key (albeit unknown) amino acid residue(s) is likely to destabilize this step, shifting the incorporation reaction back towards nucleotide release from Therminator DNA polymerase (4). The low fidelity observed with natural dNTPs supports this idea as k_{pol} is substantially higher, suggesting that both closing of the fingers domain and chemistry steps proceed with good

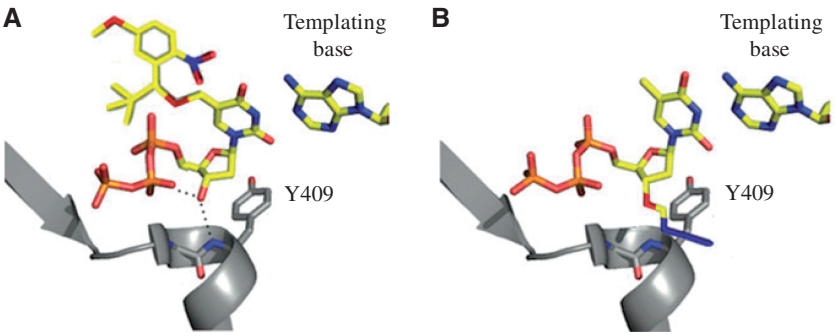

Figure 4. Models of (**A**) dU.VI and (**B**) 3′-*O*-azidomethyl-TTP interactions with Therminator DNA polymerase. The RB69 DNA polymerase ternary structure [PDB ID: 1IG9; see reference (65)] is used as a structural model for Therminator DNA polymerase and its active site [from 9°N-7 DNA polymerase (58)] was aligned with bound TTP using the pair fit function in MacPyMol (The PyMOL Molecular Graphics System, Version 1.5.0.1 Schrödinger, LLC). (A) dU.VI and (B) 3′-*O*-azidomethyl-TTP were drawn as extension of the three-dimensional structural model for TTP. Dotted lines in (A) represent hydrogen bonds between the 3′-OH group of dU.VI and its non-bridging oxygen of the β-phosphate group and –NH group of the peptide bond for Y409 (Therminator DNA polymerase amino acid numbering) that illustrate proper geometric alignment of these groups for efficient catalysis. The extension of the 3′-*O*-azidomethyl group in (B) is expected to cause a steric clash with the phenolic group side chain of Y409, thereby abolishing its incorporation efficiency. Improved incorporation performance with Therminator III, which contains the three substitutions (L408S, Y409A and P410V) that reduce the size of each amino acid side chain, supports this model.

efficiency. We cannot, however, formally rule out that the chemistry step (k_3) becomes rate limiting for the *Lightning Terminators*™ dU.V and dU.VI. In this alternative model, Therminator DNA polymerase undergoes a conformational change into the *closed* form, but the overall geometric shape of the mismatched base-pairs induce the reactive groups to be out of alignment within the active site, thus hindering the phosphoryl transfer step. Further kinetic studies are required to resolve these two models.

As noted above, the challenge of any 3′-OH unblocked terminator is the availability of this hydroxyl group for the next incoming nucleotide. Nonetheless, we present data that the common (*S*)-*tert*-butyl group attached to the α-carbon of the 2-nitrobenzyl group for dU.V and dU.VI causes absolute single-base termination (Figure 3). Because the 3′-OH is unblocked, termination of DNA synthesis is presumed to occur by a mechanism different than that of 3′-modified analogs, such as 2′,3′-ddNTPs or 3′-*O*-modified reversible terminators. At least two models can be considered to describe the modes of action that may cause DNA polymerases to terminate DNA synthesis with 3′-OH unblocked terminators: (i) misalignment model and (ii) translocation-defective model. In the misalignment model, the incoming *Lightning Terminator* is incorporated into the primer strand followed by a translocation step that allows the next incoming nucleotide to bind at the N-site (i.e. the nucleotide binding site). If the 3′-OH group of dU.V or dU.VI nucleotide is not properly aligned with the incoming nucleotide bound within the *closed* active site, then phosphoryl transfer cannot occur and synthesis halts. The translocation-defective model of termination proposes that the incoming dU.V or dU.VI is incorporated, but translocation is blocked, leaving the 3′-terminal nucleotide in the pre-translocation P-site (i.e. the primer binding site). Failure of the next incoming nucleotide to bind within the pre-translocation site results in a termination event. Previous studies by Michailidis and colleagues have demonstrated that the 3′-OH unblocked, sugar-modified nucleotide 4′-ethynyl-2-fluoro-dATP blocks human immunodeficiency virus (HIV) RT translocation and supports the translocation-defective model for termination (66). Further experimentation will be required to determine the mechanism(s) by which dU.V and dU.VI terminate DNA synthesis. Understanding how 3′-OH unblocked, base-modified nucleotides terminate synthesis could lead to new insights into polymerase mechanisms for discrimination and active site architecture and may lead to the development of a new class of effective nucleotide inhibitors as antiviral therapeutic agents.

We believe that the superior enzymatic performance properties of *Lightning Terminators*™ will have the potential to improve the performance of NGS technologies in speed, cost and accuracy. We have demonstrated that the *Lightning Terminators*™ exhibit fast nucleotide-incorporation rates, which should result in shorter cycle times with the CRT method (29,30). These fast-acting 3′-OH unblocked terminators are comparable in speed performance to the Pacific Biosciences 'real-time' nucleotides, considered to be one of the fastest chemistries currently used in NGS technologies (67,68). A major difference between these nucleotide reagents is accuracy, as the Pacific Biosciences system has been shown to have one of the highest error rates of all NGS technologies (68,69). The Illumina platform, which employs the 3′-*O*-azidomethyl terminator chemistry (34), also shows high error rates that have been attributed, at least in part, to chemistry-specific systematic errors (70). A direct comparison between Illumina and Complete Genomics (71) technologies in high coverage sequencing (~76× each platform) of the same human genome found that of the ~3.7 million single nucleotide variants called, 88% were concordant between platforms, with platform-specific calls having a high false-positive rate of at least 35% (72). Here, we have demonstrated that the *Lightning Terminators*™ dU.V and dU.VI show high fidelity in DNA synthesis compared with natural nucleotides. This enzymatic property should translate directly into improved accuracy of primary DNA sequence data. While detailed cost analysis has not been described here, we anticipate that these fast-acting, high-performance, 3′-OH unblocked *Lightning Terminators*™ will result in lower reagent usage, thus reducing a major cost component of NGS technologies. Having now developed a breadboard instrument (73), experiments are underway to demonstrate these benefits by sequencing the *E. coli* genome using the complete set of dye-labeled *Lightning Terminators*™.

SUPPLEMENTARY DATA

Supplementary Data are available at NAR Online: Supplementary Figure 1.

ACKNOWLEDGEMENTS

The authors thank Ashlee Egan, Nancy Badger and Beth Ann Cantin at NEB for their technical assistance and Sherry Metzker for critical reading of the manuscript.

FUNDING

Funding for open access charge: LaserGen, Inc.

Conflict of interest statement. The focus of LaserGen, Inc. is the commercialization of *Lightning Terminators*™, which are modified reversible terminators that have been developed by Michael L. Metzker and colleagues.

REFERENCES

1. Goodman,M.F. and Tippin,B. (2000) The expanding polymerase universe. *Nat. Rev. Mol. Cell Biol.*, **1**, 101–109.
2. Ramadan,K., Shevelev,I. and Hübscher,U. (2004) The DNA-polymerase-X family: controllers of DNA quality? *Nature Rev. Mol. Cell Biol.*, **5**, 1038–1043.
3. Berdis,A.J. (2008) DNA polymerases as therapeutic targets. *Biochemistry*, **47**, 8253–8260.
4. Johnson,K.A. (2010) The kinetic and chemical mechanism of high-fidelity DNA polymerases. *Biochim. Biophys. Acta*, **1804**, 1041–1048.
5. Hastings,P.J., Hersh,M.N., Thornton,P.C., Fonville,N.C., Slack,A., Frisch,R.L., Ray,M.P., Harris,R.S., Leal,S.M. and Rosenberg,S.M. (2010) Competition of *Escherichia coli* DNA

Polymerases I, II and III with DNA Pol IV in Stressed Cells. *PLoS one*, **5**, e10862.
6. Joyce,C.M. (1997) Choosing the right sugar: how polymerases select a nucleotide substrate. *Proc. Natl Acad. Sci. USA*, **94**, 1619–1622.
7. Steitz,T.A. (1999) DNA polymerases: structural diversity and common mechanisms. *J. Biol. Chem.*, **274**, 17395–17398.
8. Delarue,M., Poch,O., Tordo,N., Moras,D. and Argos,P. (1990) An attempt to unify the structure of polymerases. *Protein Eng.*, **3**, 461–467.
9. Gao,G., Orlova,M., Georgiadis,M.M., Hendrickson,W.A. and Goff,S.P. (1997) Conferring RNA polymerase activity to a DNA polymerase: A single residue in reverse transcriptase controls substrate selection. *Proc. Natl Acad. Sci. USA*, **94**, 407–411.
10. Astatke,M., Ng,K., Grindley,N.D.F. and Joyce,C.M. (1998) A single side chain prevents *Escherichia coli* DNA polymerase I (Klenow fragment) from incorporating ribonucleotides. *Proc. Natl Acad. Sci. USA*, **85**, 3402–3407.
11. Bonnin,A., Lázaro,J.M., Blanco,L. and Salas,M. (1999) A single tyrosine prevents insertion of ribonucleotides in the eukaryotic-type φ29 DNA polymerase. *J. Mol. Biol.*, **290**, 241–251.
12. Gardner,A.F. and Jack,W.E. (1999) Determinants of nucleotide sugar recognition in an archaeon DNA polymerase. *Nucleic Acids Res.*, **27**, 2545–2553.
13. Cases-González,C.E., Gutiérrez-Rivas,M. and Menéndez-Arias,L. (2000) Coupling ribose selection to fidelity of DNA synthesis: The role of Tyr-115 of human immunodeficiency virus type 1 reverse transcriptase. *J. Biol. Chem.*, **275**, 19759–19767.
14. Patel,P.H. and Loeb,L.A. (2000) Multiple amino acid substitutions allow DNA polymerases to synthesize RNA. *J. Biol. Chem.*, **275**, 40266–40272.
15. Yang,G., Franklin,M., Li,J., Lin,T.C. and Konigsberg,W. (2002) A conserved Tyr residue is required for sugar selectivity in a pol α DNA polymerase. *Biochemistry*, **41**, 10256–10261.
16. Reha-Krantz,L.J. and Nonay,R.L. (1994) Motif A of bacteriophage T4 DNA polymerase: role in primer extension and DNA replication fidelity. Isolation of new antimutator and mutator DNA polymerases. *J. Biol. Chem.*, **269**, 5635–5643.
17. Martín-Hernández,A.M., Domingo,E. and Menéndez-Arias,L. (1996) Human immunodeficiency virus type 1 reverse transcriptase: role of Tyr115 in deoxynucleotide binding and misinsertion fidelity of DNA synthesis. *EMBO J.*, **15**, 4434–4442.
18. Patel,P.H., Kawate,H., Adman,E., Ashbach,M. and Loeb,L.A. (2001) A single highly mutable catalytic site amino acid is critical for DNA polymerase fidelity. *J. Biol. Chem.*, **276**, 5044–5051.
19. Minnick,D.T., Liu,L., Grindley,N.D.F., Kunkel,T.A. and Joyce,C.M. (2002) Discrimination against purine-pyrimidine mispairs in the polymerase active site of DNA polymerase I: A structural explanation. *Proc. Natl Acad. Sci. USA*, **99**, 1194–1199.
20. Martín-Hernández,A.M., Gutiérrez-Rivas,M., Domingo,E. and Menéndez-Arias,L. (1997) Mispair extension fidelity of Human Immunodeficiency Virus Type 1 reverse transcriptases with amino acid substitutions affecting Tyr115. *Nucleic Acids Res.*, **25**, 1383–1389.
21. Echols,H. and Goodman,M.F. (1991) Fidelity mechanisms in DNA replication. *Ann. Rev. Biochem.*, **60**, 477–511.
22. Doublié,S., Sawaya,M.R. and Ellenberger,T. (1999) An open and closed case for all polymerases. *Structure*, **7**, R31–R35.
23. Kunkel,T.A. (2004) DNA replication fidelity. *J. Biol. Chem.*, **279**, 16895–16898.
24. Joyce,C.M. and Benkovic,S.J. (2004) DNA polymerase fidelity: Kinetics, structure, and checkpoints. *Biochemistry*, **43**, 14317–14324.
25. Astatke,M., Grindley,N.D.F. and Joyce,C.M. (1998) How *E. coli* DNA polymerase I (Klenow fragment) distinguishes between deoxy- and dideoxynucleotides. *J. Mol. Biol.*, **278**, 147–165.
26. Sanger,F., Nicklen,S. and Coulson,A.R. (1977) DNA sequencing with chain-terminating inhibitors. *Proc. Natl Acad. Sci. USA*, **74**, 5463–5467.
27. Metzker,M.L., Raghavachari,R., Richards,S., Jacutin,S.E., Civitello,A., Burgess,K. and Gibbs,R.A. (1994) Termination of DNA synthesis by novel 3'-modified deoxyribonucleoside triphosphates. *Nucleic Acids Res.*, **22**, 4259–4267.
28. Canard,B. and Sarfati,R. (1994) DNA polymerase fluorescent substrates with reversible 3'-tags. *Gene*, **148**, 1–6.
29. Metzker,M.L. (2005) Emerging technologies in DNA sequencing. *Genome Res.*, **15**, 1767–1776.
30. Metzker,M.L. (2010) Sequencing technologies — the next generation. *Nat. Rev. Genet.*, **11**, 31–46.
31. Chen,F., Gaucher,E.A., Leal,N.A., Hutter,D., Havemann,S.A., Govindarajan,S., Ortlund,E.A. and Benner,S.A. (2010) Reconstructed evolutionary adaptive paths give polymerases accepting reversible terminators for sequencing and SNP detection. *Proc. Natl Acad. Sci. USA*, **107**, 1948–1953.
32. Hutter,D., Kim,M.-J., Karalkar,N., Leal,N.A., Chen,F., Guggenheim,E., Visalakshi,V., Olejnik,J., Gordon,S. and Benner,S.A. (2010) Labeled nucleoside triphosphates with reversibly terminating aminoalkoxyl groups. *Nucleosides Nucleotides Nucleic Acids*, **29**, 879–895.
33. Guo,J., Xu,N., Li,Z., Zhang,S., Wu,J., Kim,D.H., Sano Marma,M., Meng,Q., Cao,H., Li,X. *et al.* (2008) Four-color DNA sequencing with 3'-*O*-modified nucleotide reversible terminators and chemically cleavable fluorescent dideoxynucleotides. *Proc. Natl Acad. Sci. USA*, **105**, 9145–9150.
34. Bentley,D.R., Balasubramanian,S., Swerdlow,H.P., Smith,G.P., Milton,J., Brown,C.G., Hall,K.P., Evers,D.J., Barnes,C.L., Bignell,H.R. *et al.* (2008) Accurate whole human genome sequencing using reversible terminator chemistry. *Nature*, **456**, 53–59.
35. Ju,J., Kim,D.H., Bi,L., Meng,Q., Bai,X., Li,Z., Li,X., Marma,M.S., Shi,S., Wu,J. *et al.* (2006) Four-color DNA sequencing by synthesis using cleavable fluorescent nucleotide reversible terminators. *Proc. Natl Acad. Sci. USA*, **103**, 19635–19640.
36. Wu,J., Zhang,S., Meng,Q., Cao,H., Li,Z., Li,X., Shi,S., Kim,D.H., Bi,L., Turro,N.J. *et al.* (2007) 3'-*O*-modified nucleotides as reversible terminators for pyrosequencing. *Proc. Natl Acad. Sci. USA*, **104**, 16462–16467.
37. Wu,W., Stupi,B.P., Litosh,V.A., Mansouri,D., Farley,D., Morris,S., Metzker,S. and Metzker,M.L. (2007) Termination of DNA synthesis by N^6-alkylated, not 3'-*O*-alkylated, photocleavable 2'-deoxyadenosine triphosphates. *Nucleic Acid Res.*, **35**, 6339–6349.
38. Litosh,V.A., Wu,W., Stupi,B.P., Wang,J., Morris,S.E., Hersh,M.N. and Metzker,M.L. (2011) Improved nucleotide selectivity and termination of 3'-OH unblocked reversible terminators by molecular tuning of 2-nitrobenzyl alkylated HOMedU triphosphates. *Nucleic Acid Res.*, **39**, e39.
39. Stupi,B.P., Li,H., Wang,J., Wu,W., Morris,S.E., Litosh,V.A., Muniz,J., Hersh,M.N. and Metzker,M.L. (2012) Stereochemistry of benzylic carbon substitution coupled with ring modification of 2-nitrobenzyl groups as key determinants for fast-cleaving reversible terminators. *Angew. Chem. Int. Ed.*, **51**, 1724–1727.
40. Southworth,M.W., Kong,H., Kucera,R.B., Jannasch,H.W. and Perler,F.B. (1996) Cloning of thermostable DNA polymerases from hyperthermophilic marine Archaea with emphasis on *Thermococcus* sp. 9 degrees N-7 and mutations affecting 3'-5' exonuclease activity. *Proc. Natl Acad. Sci. USA*, **93**, 5281–5285.
41. Gardner,A.F. and Jack,W.E. (2002) Acyclic and dideoxy terminator preferences denote divergent sugar recognition by archaeon and *Taq* DNA polymerase. *Nucleic Acid Res.*, **30**, 605–613.
42. Zavgorodny,S., Polianski,M., Besidsky,E., Kriukov,V., Sanin,A., Pokrovskaya,M., Gurskaya,G., Lönnberg,H. and Azhayev,A. (1991) 1-Alkylthioalkylation of nucleoside hydroxyl functions and its synthetic applications: a new versatile method in nucleoside chemistry. *Tetrahedron Lett.*, **32**, 7593–7596.
43. Metzker,M.L., Raghavachari,R., Burgess,K. and Gibbs,R.A. (1998) Elimination of residual natural nucleotides from 3'-*O*-modified-dNTP syntheses by enzymatic Mop-Up. *BioTechniques*, **25**, 814–817.
44. Benner,S.A., Hutter,D., Leal,N.A. and Chen,F. (2011), U.S. patent application 12/383,306.
45. Gardner,A.F., Joyce,C.M. and Jack,W.E. (2004) Comparative kinetics of nucleotide analog incorporation by Vent DNA polymerase. *J. Biol. Chem.*, **279**, 11834–11842.

46. Johnson,K.A. (1992) In: Sigman,D.S. (ed.), *The Enzymes*, Vol. XX, 3rd edn. Academic Press, Inc., New York, pp. 1–61.
47. Johnson,K.A. (1993) Conformational coupling in DNA polymerase fidelity. *Annu. Rev. Biochem.*, **62**, 685–713.
48. Metzker,M.L., Lu,J. and Gibbs,R.A. (1996) Electrophoretically uniform fluorescent dyes for automated DNA sequencing. *Science*, **271**, 1420–1422.
49. Chen,J.J., Tsai,C.-H., Cai,X., Horhota,A.T., McLaughlin,L.W. and Szostak,J.W. (2009) Enzymatic primer-extension with glycerol-nucleoside triphosphates on DNA templates. *PLoS One*, **4**, e4949.
50. Ichida,J.K., Horhota,A., Zou,K., McLaughlin,L.W. and Szostak,J.W. (2005) High fidelity TNA synthesis by Therminator polymerase. *Nucleic Acids Res.*, **33**, 5219–5225.
51. Kataoka,M., Kouda,Y., Sato,K., Minakawa,N. and Matsuda,A. (2011) Highly efficient enzymatic synthesis of 3'-deoxyapionucleic acid (apioNA) having the four natural nucleobases. *Chem. Commun.*, **47**, 8700–8702.
52. Kuchta,R.D., Mizrahi,V., Benkovic,P.A., Johnson,K.A. and Benkovic,S.J. (1987) Kinetic mechanism of DNA polymerase I (Klenow). *Biochemistry*, **26**, 8410–8417.
53. Brandis,J.W., Edwards,S.G. and Johnson,K.A. (1996) Slow rate of phosphodiester bond formation accounts for the strong bias that *Taq* DNA polymerase shows against 2',3'-dideoxynucleotide terminators. *Biochemistry*, **35**, 2189–2200.
54. Yang,G., Franklin,M., Li,J., Lin,T.C. and Konigsberg,W. (2002) Correlation of the kinetics of finger domain mutants in RB69 DNA polymerase with its structure. *Biochemistry*, **41**, 2526–2534.
55. Brown,J.A. and Suo,Z. (2009) Elucidating the kinetic mechanism of DNA polymerization catalyzed by *Sulfolobus solfataricus* P2 DNA polymerase B1. *Biochemistry*, **48**, 7502–7511.
56. Kennedy,E.M., Hergott,C., Dewhurst,S. and Kim,B. (2009) The mechanistic architecture of thermostable *Pyrococcus furiosus* family B DNA polymerase motif A and its interaction with the dNTP substrate. *Biochemistry*, **48**, 11161–11168.
57. Bowers,J., Mitchell,J., Beer,E., Buzby,P.R., Causey,M., Efcavitch,J.W., Jarosz,M., Krzymanska-Olejnik,E., Kung,L., Lipson,D. *et al.* (2009) Virtual terminator nucleotides for next-generation DNA sequencing. *Nat. Methods*, **6**, 593–595.
58. Rodriguez,A.C., Park,H.-W., Mao,C. and Beese,L.S. (2000) Crystal structure of a pol α family DNA polymerase from the hyperthermophilic archaeon Thermococcus sp. 9°N-7. *J. Mol. Biol.*, **299**, 447–462.
59. Zhao,Y., Jeruzalmi,D., Moarefi,I., Leighton,L., Lasken,R. and Kuriyan,J. (1999) Crystal structure of an archaebacterial DNA polymerase. *Structure*, **7**, 1189–1199.
60. Hashimoto,H., Nishioka,M., Fujiwara,S., Takagi,M., Imanaka,T., Inoue,T. and Kai,Y. (2001) Crystal structure of DNA polymerase from hyperthermophilic archaeon *Pyrococcus kodakaraensis* KOD1. *J. Mol. Biol.*, **306**, 469–477.
61. Kim,S.W., Kim,D.-U., Kim,J.K., Kang,L.-W. and Cho,H.-S. (2008) Crystal structure of *Pfu*, the high fidelity DNA polymerase from *Pyrococcus furiosus*. *Int. J. Biol. Macromol.*, **42**, 356–361.
62. Wang,J., Sattar,A.K.M.A., Wang,C.C., Karam,J.D., Konigsberg,W.H. and Steitz,T.A. (1997) Crystal structure of a pol α family replication DNA polymerase from bacteriophage RB69. *Cell*, **89**, 1087–1099.
63. Savino,C., Federici,L., Johnson,K.A., Vallone,B., Nastopoulos,V., Rossi,M., Pisani,F.M. and Tsernoglou,D. (2004) Insights into DNA replication: The crystal structure of DNA polymerase B1 from the archaeon *Sulfolobus solfataricus*. *Structure*, **12**, 2001–2008.
64. Hopfner,K.-P., Eichinger,A., Engh,R.A., Laue,F., Ankenbauer,W., Huber,R. and Angerer,B. (1999) Crystral structure of a thermostable type B DNA polymerase from *Thermococcus gorgonaritus*. *Proc. Natl Acad. Sci. USA*, **96**, 3600–3605.
65. Franklin,M.C., Wang,J. and Steitz,T.A. (2001) Structure of the replicating complex of a Pol α family DNA polymerase. *Cell*, **105**, 657–667.
66. Michailidis,E., Marchand,B., Kodama,E.N., Singh,K., Matsuoka,M., Kirby,K.A., Ryan,E.M., Sawani,A.M., Nagy,E., Ashida,N. *et al.* (2009) Mechanism of inhibition of HIV-1 reverse transcriptase by 4'-ethynyl-2-fluoro-2'-deoxyadenosine triphosphate, a translocation-defective reverse transcriptase inhibitor. *J Biol Chem*, **284**, 35681–35691.
67. Korlach,J., Bibillo,A., Wegener,J., Peluso,P., Pham,T.T., Park,I., Clark,S., Otto,G.A. and Turner,S.W. (2008) Long, processive enzymatic DNA synthesis using 100% dye-labeled terminal phosphate-linked nucleotides. *Nucleosides Nucleotides Nucleic Acids*, **27**, 1072–1082.
68. Eid,J., Fehr,A., Gray,J., Luong,K., Lyle,J., Otto,G., Peluso,P., Rank,D., Baybayan,P., Bettman,B. *et al.* (2009) Real-time DNA sequencing from single polymerase molecules. *Science*, **323**, 133–138.
69. Metzker,M.L. (2009) Sequencing in real time. *Nat. Biotechnol.*, **27**, 150–151.
70. Nakamura,K., Oshima,T., Morimoto,T., Ikeda,S., Yoshikawa,H., Shiwa,Y., Ishikawa,S., Linak,M.C., Hirai,A., Takahashi,H. *et al.* (2011) Sequence-specific error profile of Illumina sequencers. *Nucleic Acids Res.*, **39**, e90.
71. Drmanac,R., Sparks,A.B., Callow,M.J., Halpern,A.L., Burns,N.L., Kermani,B.G., Carnevali,P., Nazarenko,I., Nilsen,G.B., Yeung,G. *et al.* (2010) Human genome sequencing using unchained base reads on self-assembling DNA nanoarrays. *Science*, **327**, 78–81.
72. Lam,H.Y.K., Clark,M.J., Chen,R., Chen,R., Natsoulis,G., O'Huallachain,M., Dewey,F.E., Habegger,L., Ashley,E.A., Gerstein,M.B. *et al.* (2012) Performance comparison of whole-genome sequencing platforms. *Nat. Biotechnol.*, **30**, 78–82.
73. Hertzog,D., Hersh,M.N. and Metzker,M.L. (2011) A high-performance, low-cost approach to next-generation sequencing. *BioOptics World*, Issue Nov/Dec 2011.